In the approximations adopted here both the effective energy and the frequency are independent of temperature. This means that the Arrhenius expression for the coefficient of self-diffusion is valid:

$$D = D_i \exp(-\beta H). \tag{25}$$

Figure 3 shows the dependence of the logarithm of the coefficient of self-diffusion on pressure; note the monotonic increase of the diffusion coefficient with increasing pressure.

NOTATION

N, number of particles; V, volume of the system; $\mathbf{p}_\mu$, momentum; $\mathbf{l}_\mu$, angular momentum; m, mass of a molecule; x_μ, five-dimensional vector; $\Phi(x_\mu, x_\nu)$, molecular interaction potential; w, cell volume; β, reciprocal of the temperature; φ_i, pseudopotential; $\varphi_i(x_i)$, potential of the mean force; P, pressure; n_0, concentration of vacancies; D, coefficient of self-diffusion; k, frequency of jumps; R, length of a molecular jump; A, two-dimensional space; s_{ij}, boundary between two cells; ν, effective frequency; E, activation energy of self-diffusion; n_{ij}, unit vector; $\mathbf{e}_i$, unit orientation vector of a molecule; ε, Lennard-Jones potential well depth; r_0, linear parameter in the Lennard-Jones potential; Z_1, number of nearest neighbors.

LITERATURE CITED

1. É. T. Bruk-Levinson and O. D. Chernetsov, Inzh.-Fiz. Zh., 48, No. 5, 823-831 (1985).
2. L. A. Rott, Statistical Theory of Molecular Systems [in Russian], Moscow (1979).
3. M. V. Fedoryuk, Method of Steepest Descent [in Russian], Moscow (1977).
4. S. Chandrasekhar, "Stochastic problems in physics and astronomy," Rev. Mod. Phys., 15, 1-89 (1943).
5. H. R. Glyde, Rev. Mod. Phys. 39, No. 2, 373-382 (1967).
6. T. N. Antsygina, V. A. Slyusarev, Yu. A. Freiman, and A. I. Érenburg, Fiz. Nizk. Temp., 8, No. 2, 199-210 (1982).

OPTIMIZING HOT PRESSING FOR COLD-PRESSED POROUS BLANKS

V. B. Glasko, I. V. Demina,
S. I. Zastrozhnov, B. V. Safronov,
A. N. Tikhonov, M. K. Trubetskov,
and M. P. Shapovalov

UDC 517.9:536.2

A model is used for three-stage hot pressing, which is based on the effective characteristics for the porous cold-pressed blanks and is used to optimize the process as a whole.

1. Powder metallurgy is important because it not only economizes in metal and reduces costs but also provides composites with unique properties. Sometimes, one component here is hot pressing for cold-pressed porous blanks, in which the powder sinters.

Long sintering at high temperatures can cause selective recrystallization, or recrystallization embrittlement in the more typical refractory materials [1], i.e., strength loss, so it is necessary to control the heat treatment to obtain the necessary quality.

The control task is an inverse treatment [2], and computerized solution requires regularization [3]. A similar problem has been considered in [4] for another powder-processing technique.

Translated from Inzhenerno-Fizicheskii Zhurnal, Vol. 57, No. 1, pp. 85-90, July, 1989. Original article submitted February 22, 1988.

0022-0841/89/5701-0798$12.50

Here we give a regularized formulation of this control and a solution on the basis of a fairly simple phenomenological model.

Dynamic hot pressing involves three stages: induction heating under vacuum, cooling under vacuum during transfer to the mold, and cooling in the mold under pressure [5].

We consider a long cylindrical blank having radius R, which is infinitely extended, in an axisymmetric formulation; the heating in the first stage is in a solenoidal coil, which carries a current at a frequency ω: $I(t)\exp(i\omega t)$, in which I(t) is the slowly varying amplitude, which is taken subsequently as the control parameter.

2. Without specifying the model (see section 4), we introduce a semiempirical characteristic. One naturally assumes, which is confirmed by experiment, that the pressing quality is directly related to the temperature and time for a given mold pressure and that there is a minimal temperature u_c, the activation temperature, at which the grains sinter.

If t_2 is the initial moment in the hot pressing and T the final one, the quality of the result at a given radius r is characterized by

$$F_0(r) = \int_{t_2}^{T} \theta(u(r, t), u_c)\, dt, \quad \theta(u, v) = \begin{cases} u, & u \geqslant v, \\ 0, & u < v, \end{cases}$$

in which u(r, t) is the temperature pattern.

The region $\mathcal{R}$ with good pressing quality is specified by the following condition: the quality characteristic exceeds a certain set level $\hat{F}_0$, which is defined empirically and which is in general dependent on the equipment and pressure:

$$\mathcal{R} = \{r \in [0, R], \quad F_0(r) \geqslant \hat{F}_0\}. \tag{1}$$

This criterion is natural because the microprocess characteristics, which are largely unavailable (for diffusion, phase transformation, etc.), are largely determined by the temperature-pattern behavior.

We now consider the optimization.

3. The temperature pattern at all three stages is dependent on I(t):

$$u(r, t) = u[r, t, I(t)],$$

and we introduce the target functional

$$\Phi[I(t)] = R - r_{\max}[I(t)], \tag{2}$$

in which $r_{\max} = \sup_{r \in R} r$ is derived from (1); (2) characterizes the size of the region with inadequate sintering, and then the optimization is formulated as a turning-point treatment for I(t):

$$I(t) = \arg \inf_{I \in J} \Phi[I], \tag{3}$$

in which J is the set of constraints, which include ones on I(t) as well as ones on the temperature course. The latter are defined by the following. Firstly, during inductive heating (first stage), the temperature at any point should not exceed a preset $\hat{u}$, e.g., the melting point, recrystallization temperature, phase-transition point, etc. Secondly, when the blank is placed in the mold, the surface temperature should not exceed u_s, the temperature at which there may be reaction with the mold. This becomes very important in hot pressing for refractory and active materials such as zirconium under conditions where it is difficult to use protective lubricants.

The (3) treatment is ill-posed; the solution may be obtained by regularization as follows. We denote by K_p, p = 0, 1, ..., a set of polynomials having degree p and defined in the interval $t \in [0, t_1]$, with t_1 the instant when the first stage ends (induction heating). For each p, $I(t) \in K_p$ is governed by p + 1 parameters, the corresponding coefficients in the polynomial from the bounded set, so the K_p are compacts for any p. We consider a series of turning-point treatments

$$I(t) = \arg \inf_{I \in J \cap K_p} \Phi[I], \quad p = 0, 1, \ldots, \tag{4}$$

and choose p in accordance with the discrepancy principle [3, 6]. Here, p = 0, which corresponds to I(t) = I = const, provides a discrepancy-regularized approximation, which at the same time satisfies design simplicity.

Computational experiment showed that even the control class I(t) = I = const is extremely wide (see section 5), so one cannot merely optimize the thickness of the region giving good pressing, but also some less important criterion, as which we take the cooling time under vacuum $t_{co} = t_2 - t_1$.

Reducing t_{co} will mean not only accelerating the entire process but also a power saving, since the mean temperature level at t_1 will be lower.

The penalty-function method [7, 8] is the most natural way of incorporating the constraints on the temperature pattern in (4), which involves minimizing $\Phi[I] + \alpha(\hat{S}^2 + \check{S}^2)$ with respect to I(t), in which $\hat{S} = \max(\max\limits_{\substack{0\leqslant r\leqslant R\\ 0\leqslant t\leqslant t_1}} u(r, t) - \hat{u}, 0)$; $\check{S} = \max(u_c - \max\limits_{0\leqslant r\leqslant R} u(r, t_2), 0)$; the additional term $\hat{S}$ introduces a penalty for heating the specimen above $\hat{u}$, where $\check{S}$ is the penalty for underheating (below the activation temperature u_c) at the time t_2 when the blank is placed in the mold, and α is the parameter in the penalty-function method, which is selected during the calculations.

This approach allows one to incorporate the above criterion for minimal t_{co}; it is sufficient to add βt_{co} to the main functional, where parameter β is defined by estimating the relative cost of the functional Φ and the less important criterion t_{co}.

In this two-criterion treatment, the control task is formulated as

$$I(t) = \arg \inf_{I\in K_p} F(I), \quad F(I) \equiv \Phi[I] + \alpha(\hat{S}^2 + \check{S}^2) + \beta t_{co}, \tag{5}$$

and is solved for each p by the conjugate-direction method (Powell's method) [8, 9]; for p = 0, the (5) treatment amounts to one-dimensional minimization of F(I), which is readily done by the parabola method [9], and the resulting regularized solution is I(t) = I = const.

The algorithm for computing F(I) for each I is governed mainly by the model design, which we now consider.

4. We incorporate the actual structure under dynamic conditions at the phenomenological level by introducing effective thermophysical and electrodynamic characteristics, which are dependent on temperature and time and which can be determined for example by solving inverse-coefficient treatments [2, 3]. The explicit time dependence at the start also enables one to incorporate the pressure factor at that stage. Of course, this common method represents a highly simplified description, but one is hardly justified in complicating the model by incorporating elastoplastic strain and so on not only because the resulting boundary-value problems are complicated but also because we have very restricted information on the elastic and plastic characteristics of these powders, which are very much dependent on composition and production technology.

The amplitude H of the harmonic magnetic field induced in the specimen during the first stage is [10] defined by

$$\frac{1}{r}\frac{\partial}{\partial r}\left(\frac{r}{\lambda(u)}\frac{\partial H}{\partial r}\right) - i\omega\mu(u)\mu_0 H = 0, \quad 0 < r < R,$$
$$\left.\frac{\partial H}{\partial r}\right|_{r=0} = 0, \quad H|_{r=R} = nI(t), \tag{6}$$

in which $\lambda(u)$ and $\mu(u)$ are the effective electrical conductivity and relative magnetic permeability for the porous material, which are dependent on u, while n is the number of terms per meter on the inductor.

The thermophysical process here is described by a nonlinear boundary-value problem in thermal conduction:

$$\frac{1}{r}\frac{\partial}{\partial r}\left(rk(u)\frac{\partial u}{\partial r}\right) + \frac{1}{2\lambda(u)}\left|\frac{\partial H}{\partial r}\right|^2 = c(u)\rho(u)\frac{\partial u}{\partial t}, \quad \begin{matrix} 0 < r < R, \\ 0 < t < t_1, \end{matrix} \tag{7}$$
$$u|_{t=0} = u_0, \quad \lim_{r\to+0} rk(u)\frac{\partial u}{\partial r} = 0,$$

$$-k(u)\frac{\partial u}{\partial r}\Big|_{r=R} = \delta\sigma\left((u|_{r=R}+273{,}15)^4-(u_e+273{,}15)^4\right).$$

Here k(u), c(u), ρ(u) are the effective thermal conductivity, specific heat, and density, u_0 initial temperature, u_e environmental temperature, δ effective blackness [11], and σ Stefan's constant.

The second stage is cooling under vacuum during transfer to the mold and is described by (7) with H≡0 (no heat sources); the initial condition at $t = t_1$ is taken as the temperature pattern at the end of the first stage.

Let $k_m(u)$, $c_m(u)$, $\rho_m(u)$ be the thermophysical characteristics of the mold material in the third stage, while the characteristics of the material are k'(u), c'(u), ρ'(u); the consolidation on hot pressing is incorporated by taking the matter as explicitly dependent on time: in a time τ (a few seconds), the parameters vary linearly from the initial values (at $t = t_2$), which correspond to the porous material, to the final ones, which correspond to the dense material (at $t = t_2 + \tau$). The temperature pattern in the first stage is described by

$$\frac{1}{r}\frac{\partial}{\partial r}\left(rk'(u)\frac{\partial u}{\partial r}\right) = c'(u)\rho'(u)\frac{\partial u}{\partial t}, \quad 0<r<R,$$

$$\frac{1}{r}\frac{\partial}{\partial r}\left(rk_{\text{м}}(u)\frac{\partial u}{\partial r}\right) = c_{\text{м}}(u)\rho_{\text{м}}(u)\frac{\partial u}{\partial t}, \quad R<r<R_{\text{м}}, \quad t_2<t<T,$$

$$\lim_{r\to+0} rk'(u)\frac{\partial u}{\partial r} = 0, \quad k'(u)\frac{\partial u}{\partial r}\Big|_{r=R-0} = k_{\text{м}}(u)\frac{\partial u}{\partial r}\Big|_{r=R+0},$$

$$-k'(u)\frac{\partial u}{\partial r}\Big|_{r=R-0} = \frac{1}{R_T}(u|_{r=R-0}-u|_{r=R+0}), \quad \frac{\partial u}{\partial r}\Big|_{r=R_{\text{м}}} = 0, \tag{8}$$

in which R_m is the outer mold radius.

The initial condition at $t = t_2$ is taken as the temperature pattern at the end of the second stage ($0 < r < R$) and for $R < r < R_m$ we have $u|_{t=t_2} = u_{\text{м}}^0$ in which u_m^0 is the initial mold temperature. The linkage condition in (4) describes the gap between the specimen and the mold, thermal resistance R_T.

(6)-(8) describes the cycle and enables one to derive the temperature patterns for any given I(t) and thus the (2) and (5) functionals.

The algorithm for u(r, t; I(t)) is based on difference methods [12, 13]; for (6) and (7), one can introduce nets displaced by half a step, and then one can construct the finite-difference approximation for (6) and (7) with order $O(\Delta r^2)$ for (6) or $O(\Delta r^2 + \Delta t)$ for (7), in which Δr and Δt are the steps in r and t. Those schemes for (6) and (7) are readily solved by the pivot method with the use of an external iterative loop to incorporate the nonlinearity [10].

The nonlinear boundary condition in (7) can be written in linearized form:

$$-k(u)\frac{\partial u}{\partial r}\Big|_{r=R} = \delta\sigma\tilde{\sigma}(u|_{r=R}, u_e)(u|_{r=R}-u_e),$$

in which $\tilde{\sigma}(u, u_e) = ((u+273{,}15)^2+(u_e+273{,}15)^2)(u+u_e+2\cdot273{,}15)$, which substantially improves the convergence in the nonlinearity-iteration cycle.

One incorporates the surface temperature constraint on mold placing in realization by choosing t_2 from $u(R, t_2)\leqslant u_s$.

5. We now report some results obtained with a BÉSM-6 on a program that implements the algorithms in sections 2-4, which relate to a model having the following parameters: R = 0.05 m, R_m = 0.15 m, $\omega = 2\pi\cdot2.4$ kHz, n = 100 m^{-1}, δ = 0.3, u_0 = 500°C, u_e = 20°C, $R_T = 3.3\cdot10^{-5}$ $m^2\cdot°C/W$, t_1 = 300 sec, u_c = 850°C, u_s = 900°C, u_m^0 = 200°C, $\hat{u}$ = 1300°C, $\hat{F}_0$ = 4000°C·sec.

Figure 1 shows the temperature dependence of the characteristics for the mold and specimen materials (μ(u) = 1, c_m = 134 J/(kg·°C), ρ_m = 19350 kg/m^3); if ε = 0.2 is the bulk porosity, the thermal and electrical conductivities can be derived subject to certain

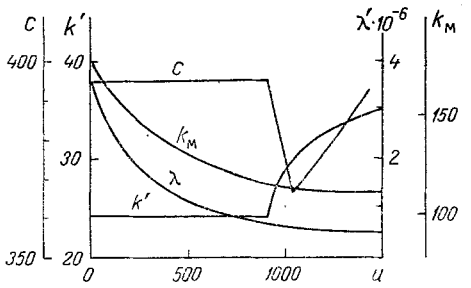

Fig. 1

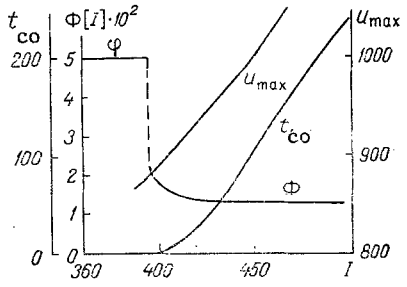

Fig. 2

Fig. 1. Dependence on temperature u (°C) for the mold thermal conductivity k_m, W/m·°C, and of the blank thermal conductivity k' in the same units, electrical conductivity λ in $(\Omega \cdot m)^{-1}$, and specific heat c in J/°C·kg.

Fig. 2. Effects of current amplitude I in A on the thickness Φ of the region with poor pressing quality in m and on the maximum blank temperature u_{max} in °C and the vacuum cooling time t_{co} in sec.

assumptions from $k(u)=k'(u)\ K$, $\lambda(u)=\lambda'(u)\ K$ in which $K = 2(1 - \varepsilon)/(2 + \varepsilon)$ [14]; the density is $\rho(u) = \rho'(u)(1 - \varepsilon)$, $\rho'(u) = 6500$ kg/m³.

Figure 2 shows the dependence on I for $\Phi[I]$, $t_{co}[I]$ and $u_{max}[I] = \max\limits_{\substack{0\leqslant r\leqslant R\\ 0\leqslant t\leqslant t_1}} u(r, t)$; for $I \leq 400$ A, $\Phi[I] = R$, which means no pressing. As I increases, the process starts, and $\Phi[I]$ falls stepwise and tends to a shallow minimum. For $I > 430$ A, the current has no appreciable effect on $\Phi[I]$, but t_{co} and u_{max} continue to increase with I, which shows that simultaneous optimization on t_{co} is possible.

We solved (5) with β chosen in the numerical experiment from the estimator for the maximal value $\hat{t}_{co} = \sup\limits_{I\in J} t_{co}[I]$, the minimal value $\Phi^* = \inf\limits_{I\in J} \Phi[I]$ and the relation $\beta\hat{t}_{co} = 0{,}1\Phi^*$ which characterizes the relative costs of the optimization criteria. This gave $\beta = 10^{-5}$ ($\Phi^* \sim 10^{-2}$ m, $\hat{t}_{co} \sim 100$ sec); here the choice of α is not so critical, since varying it influences only the minimization-algorithm convergence rate since the optimum control lies within the region of the constraints J and the penalties $\check{S}$ and $\hat{S}$ become zero for it.

This optimization algorithm provides the optimum I under automatic control, and the center of the specimen is well pressed.

These results show that the method is effective for this process; the same approach can give the optimization for a more complicated model if one has adequate information on the powder's physical parameters.

LITERATURE CITED

1. V. V. Skorokhod and S. M. Solonin, The Physical and Metallurgical Principles of Powder Sintering [in Russian], Moscow (1984).
2. V. B. Glasko, Inverse Treatments in Mathematical Physics [in Russian], Moscow (1984).
3. A. N. Tikhonov and V. Ya. Arsenin, Methods of Solving Ill-Posed Problems [in Russian], Moscow (1979).
4. E. A. Vishnevskaya, V. B. Glasko, M. K. Trubetskov, and S. G. Popov, Inzh.-Fiz. Zh., 50, No. 5, 835-839 (1986).
5. Yu. G. Dorofeev, Dynamic Hot Pressing for Porous Powder Blanks [in Russian], Moscow (1977).
6. A. S. Leonov, Dokl. Akad. Nauk SSSR, 262, No. 6, 1306-1310 (1982).
7. F. P. Vasil'ev, Methods of Solving Turning-Point Problems [in Russian], Moscow (1981).
8. B. N. Pshenichnyi and Yu. M. Danilin, Numerical Methods in Turning-Point Problems [in Russian], Moscow (1975).
9. D. Himmelblau, Applied Nonlinear Programming [Russian translation], Moscow (1975).

10. V. B. Glasko, N. I. Kulik, A. N. Tikhonov, and I. N. Shklyarov, Zh. Vychisl. Mat. Mat. Fiz., 19, No. 3, 768-774 (1979).
11. G. Greber, S. Erk, and U. Griguos, The Principles of Heat Transfer [Russian translation], Moscow (1958).
12. A. A. Samarskii, Difference-Scheme Theory [in Russian], Moscow (1983).
13. N. N. Kalitkin, Numerical Methods [in Russian], Moscow (1978).
14. G. N. Dul'nev and Yu. P. Zarichnyak, The Thermal Conductivities of Mixtures and Composites (Handbook) [in Russian], Leningrad (1974).

NUMERICAL STUDY OF THE NONEQUILIBRIUM FILTRATION OF IMMISCIBLE LIQUIDS

O. B. Bocharov, V. V. Kuznetsov, and Yu. V. Chekhovich

UDC 532.546

The uniform displacement of immiscible liquids in a porous medium is studied numerically for two difference methods of accounting for nonequilibrium.

The classical theory of equilibrium filtration of immiscible liquids constructed by Masket and Leverett is based on the function of relative phase permeabilities $K_i(s)$ and the Leverett function $J(s)$, characterizing the capillary pressure jump. These functions were established from experiments on steady-state displacement. The nonsteady displacement process is usually characterized by the presence of regions of sharp change in saturation with respect to both space and time, the Masket–Leverett equilibrium theory sometimes being invalid in this case. The simplest scheme of allowance for nonequilibrium [1] reduces to assuming that the functions $K_1(s)$ and $K_2(s)$, $J(s)$ are the same in a nonequilibrium flow as in the equilibrium case but depend not on the true water saturation s but on a certain effective water saturation σ. The authors of [2] proposed a kinetic equation linking the effective saturation with the true saturation:

$$\sigma = s + \tau(s)\frac{\partial s}{\partial t}. \tag{1}$$

The methods of asymptotic analysis were used in [2] to obtain the dependence of the width of the displacement front on velocity for this model with $\tau(s) = \text{const}$, while the problem of countercurrent capillary impregnation was analyzed in [3]. The problem of displacement with large values of the nonequilibrium parameter has not yet been investigated. At the same time, the effect of nonequilibrium on displacement characteristics may be great in the flooding of oil-bearing strata [4].

Here, we use a unidimensional formulation to numerically analyze displacement with a constant total flow of fluids into the sample (Rappaport–Lees problem) within the framework of a model of nonequilibrium filtration with $\tau(s)$ monotonically increasing from 0 to τ_* and $s \in [0, s_*]$.

At a constant rate of filtration of the mixture V_0, the system of Masket–Leverett equations and Eq. (1) reduce to the following dimensionless equations (with the same notation being kept for the dimensionless variables):

$$\frac{\partial s}{\partial t} = \frac{\partial}{\partial x}\left[\varepsilon a(\sigma)\frac{\partial \sigma}{\partial x} - F(\sigma)\right], \tag{2}$$

$$DR(s)\frac{\partial s}{\partial t} + s = \sigma. \tag{3}$$

Here, $D = \tau_* V_0/Lm$; $\mu = \mu_1/\mu_2$; $\varepsilon = \gamma\sqrt{Km}/V_0 L\mu_2$; $F(\sigma) = K_1(\sigma)/(K_1(\sigma) + \mu K_2(\sigma))$; $a(\sigma) = -F(\sigma)K_2(\sigma)\dfrac{dJ(\sigma)}{d\sigma}$;

All-Union Oil and Gas Scientific Research Institute. Translated from Inzhenerno-Fizicheskii Zhurnal, Vol. 57, No. 1, pp. 91-95, July, 1989. Original article submitted January 4, 1988.

0022-0841/89/5701-0803$12.50